

# Dynamics in a supercooled molecular liquid: Theory and Simulations

A. Rinaldi, F. Sciortino and P. Tartaglia

*Dipartimento di Fisica and Istituto Nazionale per la Fisica della Materia, Università di Roma La Sapienza,  
P.le Aldo Moro 2, I-00185, Roma, Italy*

(November 12, 2018)

We report extensive simulations of liquid supercooled states for a simple three-sites molecular model, introduced by Lewis and Wahnström [L. J. Lewis and G. Wahnström, Phys. Rev. E **50**, 3865 (1994)] to mimic the behavior of *ortho*-terphenyl. The large system size and the long simulation length allow to calculate very precisely — in a large  $q$ -vector range — self and collective correlation functions, providing a clean and simple reference model for theoretical descriptions of molecular liquids in supercooled states. The time and wavevector dependence of the site-site correlation functions are compared with detailed predictions based on ideal mode-coupling theory, neglecting the molecular constraints. Except for the wavevector region where the dynamics is controlled by the center of mass (around  $9 \text{ nm}^{-1}$ ), the theoretical predictions compare very well with the simulation data.

## I. INTRODUCTION

In the last decade, increased computational resources have been used to tackle the study of the onset of glassy dynamics [1–8], one of the most interesting open problems in the physics of liquids. Supercooled liquids are indeed characterized by an extreme  $T$ -dependence of the structural times, which covers more than 15 orders of magnitude in a small temperature interval. Present computer facilities allow to follow the change in the structure and in the dynamics of the system (in equilibrium) over a  $T$  range where the diffusivity changes more than 5 order of magnitudes. At the same time, computer simulations are starting to provide a detailed picture of the structure of the potential energy landscape probed in supercooled states [9–14]. The calculated trajectories offer an outstanding possibility for studying the origin of the slowing down of the dynamics, and call for a careful comparison between theories and “exact” numerical calculations.

“Exact” results calculated for model-system and theoretical predictions based on mode coupling theory (MCT) [15,16] have been reported for several atomic liquids, — encompassing hard spheres, soft spheres, Lennard-Jones [2], and recently silica [17]. In the case of molecular liquids, where the possibility of comparing with experiments makes the effort even more valuable, molecular dynamics (MD) simulations extending to the 100  $ns$  timescale are now possible. Detailed comparisons between theories and simulations appears as well [18–21].

MD simulations have often been used to generate reference systems for validating theories of liquids, starting

from the pioneering work of Alder and Wainwright [22] on hard spheres. A very interesting model for a molecular liquid was designed by Lewis and Wahnström (LW) [23] by gluing in a rigid molecule three identical Lennard-Jones (LJ) atoms. The shape of the molecule (an isosceles triangle) and the LJ parameters were chosen to mimic as close as possible one of the most studied glass-forming, liquid [24–31] *ortho*-terphenyl (OTP). This model provides a clean bridge between studies based on atomic LJ potentials and more complex molecular potentials. From a theoretical point of view, such a model is also very valuable, since the LW model lends itself to several approximation of increasing complexity. For example, one could consider the LW system as a liquid of identical atoms, correlated in space according to the site-site correlation function (without differentiating between intra and intermolecular sites), or one can improve by including the molecular correlation via the triplet site-site-site correlations. Solution of the exact molecular model, implementing a site-site description [32] which accounts for the intramolecular constraints or an expansion in generalized spherical harmonics [33,34] is also foreseeable.

The LW potential was introduced in Ref. [23], which reports a study of the slow dynamics of the LW liquid. The major properties of such models were discussed both for self and collective properties. In following papers [35], LW made also some preliminary attempts to describe the intermediate time dynamics using MCT predictions. Favored by the increased computational power, we have decided to revisit such a model and — by extending the simulation time by a factor 20 and the number of molecules by a factor 30 — to calculate detailed properties of the dynamics in supercooled states, like the non ergodicity parameters for both self, collective and orientational properties to be used as reference system to be compared with theoretical predictions. We present such data in this article. We also solve the MCT equations for such a model using as input the site-site structure factor and the site-site-site triplet correlation functions calculated from the simulated trajectories. The comparison between the molecular dynamics data and the MCT predictions is very valuable in assessing the role of the center of mass dynamics (which is neglected in the chosen MCT approach), the role of the triplet correlations [36,17] and, in general, the ability of ideal MCT to capture the dynamics of molecular liquids in weakly supercooled states.

## II. THE MODEL AND NUMERICS

The geometry of the LW molecule is a rigid three sites isoscele triangle hosting on each site a Lennard Jones atom. The site-site spherical potentials is

$$V(r) = 4\epsilon \left( \left( \frac{\sigma}{r} \right)^{12} - \left( \frac{\sigma}{r} \right)^6 \right) + A + B r \quad (1)$$

with  $\epsilon = 5.276 \text{ kJ/mol}$ ,  $\sigma = 0.4828 \text{ nm}$ ,  $A = 0.4612 \text{ kJ/mol}$  and  $B = -0.3132 \text{ kJ/mol/nm}$ . The parameters of the potential have been selected to reproduce bulk properties of the OTP molecule [23]. The value of  $A$  and  $B$  has been selected to bring the potential and its first derivative to zero at  $r = 1.2616 \text{ nm}$ . The resulting potential has a minimum at  $r = 0.5421 \text{ nm}$  of depth  $-4.985 \text{ kJ/mol}$ . The length of the two short sides is  $0.483 \text{ nm}$  and of the long side  $0.588 \text{ nm}$ , forming an isoscele angle of 75 degrees.

We have studied a system composed by  $N = 9261$  molecules for several state points, from  $T = 255 \text{ K}$  to  $T = 346 \text{ K}$ , as listed in Table I. The choice of a large system size was performed to avoid spurious oscillations in the correlation functions introduced by the periodic boundary conditions. The large size was also preferred to access information — here and in future analysis — on the small wavevector dynamical behavior.

In this article we discuss in detail the auto correlation function for the collective and self density operators, both for center of mass (COM) and sites (s). The density operators  $\rho$  (and their corresponding autocorrelation functions) are defined as [37]

$$\rho_{COM}(\mathbf{q}) \equiv \frac{1}{\sqrt{N}} \sum_{i=1}^N e^{i\mathbf{q}\cdot\mathbf{r}_{COM}^i};$$

$$F_{COM}(\mathbf{q}, t) \equiv \langle \rho_{COM}(\mathbf{q}, t) \rho_{COM}(\mathbf{q}, 0)^* \rangle \quad (2)$$

$$\rho_s(\mathbf{q}) \equiv \frac{1}{\sqrt{3N}} \sum_{i=1}^N \sum_{j=1}^3 e^{i\mathbf{q}\cdot\mathbf{r}_j^i}; \quad F_s(\mathbf{q}, t) \equiv \langle \rho_s(\mathbf{q}, t) \rho_s(\mathbf{q}, 0)^* \rangle \quad (3)$$

$$\rho_{COM}^{self}(\mathbf{q}) \equiv e^{i\mathbf{q}\cdot\mathbf{r}_{COM}^i};$$

$$F_{COM}^{self}(\mathbf{q}, t) \equiv \langle \rho_{COM}^{self}(\mathbf{q}, t) \rho_{COM}^{self}(\mathbf{q}, 0)^* \rangle \quad (4)$$

$$\rho_s^{self}(\mathbf{q}) \equiv e^{i\mathbf{q}\cdot\mathbf{r}_j^i}; \quad F_s^{self}(\mathbf{q}, t) \equiv \langle \rho_s^{self}(\mathbf{q}, t) \rho_s^{self}(\mathbf{q}, 0)^* \rangle \quad (5)$$

where  $\mathbf{r}_{COM}^i$  and  $\mathbf{r}_j^i$  are the position of the COM and of the  $j$ -site of molecule  $i$ . Moreover,  $S_{COM}(q) \equiv F_{COM}(q, 0)$  and  $S_s(q) \equiv F_s(q, 0)$  are the COM and site static structure factors.

We also present the  $l$ -dependent rotational correlators for the molecule symmetry axis  $\mu$ , defined as

$$C_l(t) \equiv \langle P_l[\cos\theta(t)] \rangle \quad (6)$$

where  $\theta(t) = \cos^{-1}[\langle \mu(t) \cdot \mu(0) \rangle / \langle \mu(0) \cdot \mu(0) \rangle]$  and  $P_l$  is the  $l$ -order Legendre polynomial. The triplet site-site-site correlation function  $c_3(\mathbf{k}, \mathbf{p}, \mathbf{q})$  defined as

$$\begin{aligned} & \langle \rho_s(\mathbf{k}) \rho_s(\mathbf{p}) \rho_s(\mathbf{q}) \rangle \\ &= 3N S_s(k) S_s(p) S_s(q) \delta_{\mathbf{q}, \mathbf{k}+\mathbf{p}} (1 + n^2 c_3(\mathbf{k}, \mathbf{p}, \mathbf{q})) \end{aligned} \quad (7)$$

has been calculated evaluating the left hand side of Eq. 7;  $n$  is the site number density. The evaluation of  $c_3$  has been performed at  $T = 266 \text{ K}$  averaging over 1000 independent configurations, spanning a time interval of 75 ns. Where possible, up to 300 different triplets of wavevectors with the same moduli and relative angles have been averaged. We have calculated  $c_3$  for moduli of  $\mathbf{k}, \mathbf{p}$  and  $\mathbf{q}$  less than  $44.4 \text{ nm}^{-1}$  with a mesh of  $0.44 \text{ nm}^{-1}$ .

## III. MODE COUPLING APPROXIMATIONS

In this article we present two theoretical calculations of the dynamics of the sites. The first approximation neglects completely the presence of the molecular constraints and assumes that the site-site structure factor includes all requested information on the structure of the liquid. This strong approximation allows to apply in a straightforward manner the MCT equation for simple liquids. According to MCT the time evolution of the normalized collective density correlation functions  $\Phi_q(t)$  is given by

$$\ddot{\Phi}_q(t) + \nu_q \dot{\Phi}_q(t) + \Omega_q^2 \Phi_q(t) + \Omega_q^2 \int_0^t ds m_q(t-s) \dot{\Phi}_q(s) = 0. \quad (8)$$

Here  $\Omega_q = \sqrt{qv/S_s(q)}$ , with  $v$  denoting the thermal velocity, is an effective phonon-dispersion law and  $\nu_q = \nu_1 q^2$  denotes a damping constant. The kernel  $m_q$  is given as  $m_q(t) = \mathcal{F}_q(\{\Phi_k(t)\})$ , where the mode-coupling functional  $\mathcal{F}_q$  is determined by the structure factor:

$$\mathcal{F}_q(\{f_k\}) = \frac{1}{2} \int \frac{d^3k}{(2\pi)^3} V_{\mathbf{q}, \mathbf{k}} f_k f_{|\mathbf{q}-\mathbf{k}|}, \quad (9)$$

$$V_{\mathbf{q}, \mathbf{k}} \equiv S_s(q) S_s(k) S_s(|\mathbf{q}-\mathbf{k}|) \frac{n}{q^4} [\mathbf{q} \cdot \mathbf{k} c_k + \mathbf{q} \cdot (\mathbf{q}-\mathbf{k}) c_{|\mathbf{q}-\mathbf{k}|}]^2. \quad (10)$$

where  $c_q = (1 - S_s(q)^{-1})/n$  is the direct correlation function in  $q$ -space.

The second approximation is devised to retain some of the information of the molecular shape through the

inclusion of the triplet correlation function  $c_3$  [36], previously assumed to be zero. The memory function is then given by

$$V_{\mathbf{q},\mathbf{k}} \equiv S_s(q)S_s(k)S_s(|\mathbf{q}-\mathbf{k}|)\frac{n}{q^4} [\mathbf{q}\cdot\mathbf{k}c_k + \mathbf{q}\cdot(\mathbf{q}-\mathbf{k})c_{|\mathbf{q}-\mathbf{k}|} - q^2n c_3(\mathbf{q},\mathbf{k},\mathbf{q}-\mathbf{k})]^2. \quad (11)$$

For simple atomic liquids, previous studies [36] have shown that the approximation  $c_3 = 0$  does not modify the MCT predictions, except for a small shift in the estimate of the critical temperature. Recently, it has been shown [17] that in network forming liquids, the  $c_3$  contributions play a crucial role. Including the  $c_3$  contributions could, in the present case, be relevant for describing the intramolecular site-site relations. For this reason, we compare the numerical data with both predictions.

We numerically solved Eq. 8 on a grid of 300 equally spaced  $q$  values extending up to  $q = 120 \text{ nm}^{-1}$ , implementing the efficient techniques described in Ref. [38]. The long time limit of  $\Phi_q(t)$  at the dynamical critical temperature — the so-called non ergodicity parameter —  $f_q$  is obtained by an iterative solution of the bifurcation equation

$$\frac{f_q}{1-f_q} = \mathcal{F}_q(\{f_k\}). \quad (12)$$

Close to the critical point, 20000 iterations were requested to solve Eq.12 with a precision of  $10^{-15}$ . We have solved Eqs.8 for both approximations. The estimated critical temperatures are  $T = 152 \text{ K}$  and  $T = 340 \text{ K}$  for the two approximations. Thus, neglecting completely the molecular constraints (first approximation) strongly weakens the vertex function, resulting in a theoretical critical temperature lower than the numerical  $T_{MD}^c$ . Including the triplet correlation moves up the critical temperature by a factor bigger than 2, resulting in an overestimation of the critical temperature, as always found in all previous MCT calculations. Notwithstanding the large difference in critical temperature the exponent parameter [15] is  $\lambda = 0.70$  in both approximations, corresponding to the exponents  $b = 0.64$  and  $a = 0.32$  [15].

## IV. MOLECULAR DYNAMICS RESULTS

### A. Static

The site and COM static structure factors are shown in Fig. 1, as a function of temperature. The COM structure factor does not show any appreciable change with  $T$ . Instead, the site structure factor increases significantly at the first peak position (corresponding in real space to the site-site nearest neighbor distance), consistently with the behavior of simple liquids. The absence of any change in

the COM structure factor shows that the slowing down of the dynamics in this model is controlled by the changes in orientational order. It is the ordering process in the orientational degrees of freedom which drives the slowing down of the dynamics. Any theoretical approach attempting to predict the slow-dynamics in this model must require orientational (or site-site) static information as input. The absence of any  $T$ -dependence in the COM structure factor, except for the very clear reduction of the compressibility on cooling (see below), suggest the possibility that  $T$ -independent peaks in the experimentally measured OTP structure factor are associated to COM features. Of course, the present model does not allow a straightforward comparison with experimental data (as performed for example in Ref. [39]), since proton and carbon atoms are not explicitly taken into account.

The large simulation box allows to precisely calculate the  $q \rightarrow 0$  limit of the structure factor. As expected, we find that  $S_{COM}(q \rightarrow 0) = S_s(q \rightarrow 0)/3$ . The  $T$ -dependence of  $S_s(q \rightarrow 0)$  is shown in the inset of Fig. 1.

### B. Self-Dynamics

Fig. 2 shows the  $T$  dependence of the diffusion coefficient  $D$ , evaluated from the long time behavior of the mean square displacement. Compared to the LW original data, the range of  $T$  where equilibrium states has been simulated is larger and the precision in the determination of the values of  $D$  is improved. The larger  $T$ -range shows that two regions, which differ in the  $T$ -dependence of  $D$ , are observed. Above  $T = 275 \text{ K}$ ,  $D(T)$  is consistent with a power law behavior in  $T - T_{MD}^c$ , with  $T_{MD}^c = (265 \pm 1) \text{ K}$  and exponent  $\gamma = 2.0 \pm 0.1$ . Below  $T = 275 \text{ K}$ ,  $D$  decreases on a slower pace, which could be approximated with an Arrhenius law. The two different behaviors reflect the dynamics differences associated to the region of validity of MCT ( $T > T_{MD}^c$ ) and to the region ( $T < T_{MD}^c$ ) where hopping phenomena become relevant. The change in dynamical behavior shows up already for  $|T - T_{MD}^c|/T_{MD}^c = 0.06$ , confirming the general expectation that hopping phenomena may mask the critical dynamics close to the critical MCT temperature. As discussed at length in Ref. [40], the presence of hopping phenomena in this model makes impossible a clear-cut identification of the critical dynamics, without making use of information provided by the  $T$ -dependence of the  $\alpha$ -relaxation phenomenon. Similar changes in dynamical behavior close to the critical MCT temperature have been recently reported in models of silica [41] and water [42]. It is worth noting that in the original work of LW, hopping phenomena in the orientational degrees of freedom were detected starting from  $T = 266 \text{ K}$ .

The temperature dependence of the site self-correlation function  $F_s^{self}$  is reported for a specific wavevector in

Fig. 3. Similar figures characterize the time dependence of  $F_s^{self}$  at different values of  $q$ . The change in dynamics above and below  $T_{MD}^c$  can be observed also in the so-called time- $T$  superposition graph, where curves for the same correlator are shown as a function of a scaled time. Indeed, in the  $\alpha$ -relaxation region the so-called time-temperature superposition principle states that it is possible to represent the  $T$ -dependence of an arbitrary correlator  $\phi(t)$  on a single master curve, by rescaling the time via a single  $T$ -dependent timescale, i.e.

$$\phi(t) = \phi(t/\tau(T)) \quad (13)$$

The scaling time  $\tau(T)$  is conveniently defined [1] as the time when the correlation function has decayed to an arbitrary chosen value, for example  $1/e$ . Fig. 4 shows the time- $T$  superposition for the *COM* self density correlation function both above and below (inset)  $T_{MCT}$ . Only for  $T \geq 275 K$ , where  $D$  is well described by a power-law, the time- $T$  superposition principle is well obeyed. Below  $275 K$ , deviations start to be noticeable and the plateau value starts to increase.

To describe in a compact way the  $q$  dependence of the  $\alpha$ -relaxation and to make contact with the theoretical and experimental evaluations, we present in the next two figures the parameters which better describe the self density-density correlation functions according to the Von Schweidler law and the stretched exponential form. For a generic correlation function  $\phi(t)$ , the Von Schweidler law,

$$\phi(t) = f_c - h_{(1)}(t/\tau)^b + h_{(2)}(t/\tau)^{2b} + O((t/\tau)^{3b}) \quad (14)$$

describes, including the next to leading order corrections, the departure from the plateau value  $f_c$  in the early  $\alpha$ -relaxation region. The amplitudes  $h_{(1)}$  and  $h_{(2)}$  strongly depend on the physical features of the studied liquid and have been explicitly calculated within MCT for several models (see for example for hard spheres [43]). The  $\alpha$ -relaxation time scale  $\tau$  is a temperature dependent parameter which, according to MCT, scales as the inverse of diffusivity

$$\tau(T) \sim |T - T_c|^{-\gamma} \quad (15)$$

The exponent  $b$  is fixed by the value of  $\gamma$  [15]. The Kohlrausch-Williams-Watts stretched exponential form

$$\phi(t) = A_K e^{-\left(\frac{t}{\tau_K}\right)^{\beta_K}} \quad (16)$$

is often used to empirically fit the last part of the  $\phi(t)$  decay.

Since all correlation functions obey the time-temperature superposition principle, the parameters of the two functional forms are calculated by fitting the  $T = 275 K$  correlation function in the time interval  $30 < t < 600 ps$  for the Von Schweidler law and in

the time interval  $t > 20 ps$  for the stretched exponential form. Similar results are obtained by fitting the  $T = 266 K$  data. The fit of the data according to Eq. 14 has been performed by constraining the exponent  $b$  to two different values: the value  $b = 0.64$ , obtained theoretically in Sec. III for both approximations and the value  $b = 0.77$  consistent with the exponent  $\gamma$  extracted from the analysis of the diffusivity data. The fitting parameters  $f_c$  does not depend on the value of  $b$ . Except for a  $q$ -independent multiplicative factor, also the  $q$ -dependence of  $h_1$  is independent of the choice of  $b$ .

Fig. 5 shows the  $q$ -dependence of the fitting parameters according to Eq. 14. In the case of the self correlation function, the non-ergodicity parameter  $f_c(q)$  provides a description, in  $q$ -space, of the confining cage. The width of the COM cage is larger than the site one, supporting the view that the site experience an additional delocalization associated to the hindered librational motions. Moreover, we note that the site non-ergodicity parameter is not described by a simple gaussian in  $q$ -space. The  $q$ -dependence of  $h_1$  and  $h_2$  follows the oscillation of the corresponding static structure factor.

Fig. 6 shows the fitting parameters according to Eq. 16. At small wavevectors the extremely long decay of the correlation function, controlled by the diffusion of the molecules over distances of the order of  $q^{-1}$  does not allow an unbiased determination of the fitting parameters. From the wavevector range where the fitting parameters are reliable, one can notice that, as commonly found,  $A_k$  mimics  $f_q$ , that  $\beta$  goes to 1 at small  $q$  and that the product  $Dq^2\tau$  has a weak  $q$ -dependence.

We also report the rotational dynamics of the LW molecule along the symmetry axis. Fig. 7(top) shows the time dependence of the first five Legendre polynomials. We also show the corresponding fit with the the stretched exponential and the Von Schweidler law. For all angular correlators, the time-temperature superposition principle holds beautifully, as shown in Fig. 7(bottom). Since the quality of the data is very good, even tiny discrepancies would be visible. For completeness, we report also the fitting parameters according to the functional forms of Eqs. 14-16 in Figs. 8-9. The monotonic behavior of the fitting parameters in  $l$  suggests that for the LW potential, the scenario for the rotational dynamics is of the strong hindrance type [44], as found also for the case of SPC/E water [45,46].

The theoretical prediction of the wavevector dependence of the quantities reported in Figs. 5,6,8 and 9 is one of the major challenge to the recent proposed molecular mode coupling theories [47,32,33].

### C. Collective Dynamics

The collective density fluctuations are particularly relevant in the description of liquids dynamics. The non-

monotonic wavevector dependence of the characteristic times provides indication of the different timescale of the structural modes of the system and their connection with the system characteristic lengths.

We start discussing the site-site correlation functions, which can be compared with the corresponding correlation functions calculated according to MCT, as discussed in Sec. III. In comparing with the Von Schweidler and the stretched exponential parameterizations, the solutions of the MCT equations (with and without the  $c_3$  contribution), have been treated similarly to the MD data. Fig. 13 shows the  $q$ -dependence of the stretched exponential parameters,  $A_K$ ,  $\beta_K$  and  $\tau_K$ . We note that the theory captures the  $q$ -dependence of the  $\alpha$ -relaxation phenomenon close to the maximum of the site-site structure factor. The large wavevector region is also described in a reasonable way. The theory fails in describing the non-ergodicity parameters in the region where the COM structure factor has his peak position. The slowest modes in the system are indeed located around  $9 \text{ nm}^{-1}$  ( $S_{COM}$  peak position) and around  $15 \text{ nm}^{-1}$  ( $S_s$  peak position). The role of the center of mass static correlation in controlling the molecular dynamics has been observed in recent experimental studies on supercooled molecular liquids [48].

The slowing down of the dynamics in the very low- $q$  region, below the region of influence of the COM, is also predicted in a reasonable way by the site MCT developed in Sec. III. The stretching exponent parameter  $\beta_K$  is the one which seems to suffer more by the chosen approximations, which neglects the site-site intramolecular constraints. Indeed, the theoretical estimate is always higher than the MD results. The prediction of a higher value of  $\beta$  is consistent with the reduced number of vertices included in the chosen MCT approach. A more elaborate approach would require as input a large number of angular static structure factor correlators [49] (which for the present molecule would make the theory difficult to solve numerically) or the site-site partial static structure factors, discriminating at least between the central and the two external sites. The development of the molecular and site-site MCT approaches is taking place in the present days and we look forward applying them to the LW model.

To substantiate the hypothesis that the disagreement between theory and MD data in the region around  $9 \text{ nm}^{-1}$  arises from the approximation used, which neglects the constraints among sites due to the intramolecular bonding, we compare in Fig. 14 the de Gennes predictions for the COM and site correlation times with the corresponding MD data (from Fig. 13). It is clearly seen that the dynamics in the wavevector region around  $9 \text{ nm}^{-1}$  is indeed controlled by the COM static structure factor [50].

We next compare in Fig. 10 and 11 the prediction of MCT for the non ergodicity parameter and for the am-

plitude of the Von Schweidler law with the MD results. Again, we notice that the theoretical predictions satisfactorily describe the MD data except for the region where the COM structure factor has its maximum. Including the  $c_3$  contribution improves the agreement in the hydrodynamic limit. Around the peak position of  $S_s(q)$ , the agreement is very good, considering that neither fitting nor scaling parameters are involved in the comparison. In this wavevector region, the long-time dependence of the collective site-site correlation function  $F_s(q, t)$  is rather well predicted by the theory, as shown in Fig. 12.

We now turn to the COM correlators. These functions cannot be compared with the theoretical predictions reported in Sec.III, since this approximation neglects the molecular constraints. But the  $q$ -dependence of the COM correlators is very relevant for comparisons with future molecular MCT predictions. Figs. 15 and 16 show the parameterization of the COM collective  $\alpha$ -relaxation using Eqs. 16 and 14. The rather featureless shape of the COM structure, which as seen in Fig. 1 shows only a broad peak around  $9 \text{ nm}^{-1}$ , carries on to the  $q$ -dependence of all fitting parameters.

## V. CONCLUSIONS

The present study of the simple molecular model, introduced by Lewis and Wahnström to mimic the behavior of *ortho*-terphenyl, provides a clean and simple reference model for theoretical descriptions of the dynamics of molecular liquids in supercooled states.

The simple MCT analysis reported in this article and compared in detail with the MD data shows that already the MCT equations for atomic liquids are able to provide a rather accurate description of the site dynamics, except for the region around  $9 \text{ nm}^{-1}$  where the COM dynamics is dominant. We have provided evidence that, in this region, the center of mass fully controls the slow-dynamics in the liquid [50]. Taking into account the triplet correlation function  $c_3$  is shown to improve significantly only the small wavevector region. This is not surprising, since the usually employed approximation  $c_3 = 0$  fails badly at small wavevectors [51]. While this is not a major issue in the intermediate wavevector range (i.e. for the caging physics) it will become an important element in the attempt to extend (toward long wavelengths) the theoretical predictions.

The present theoretical work, which can be considered a zeroth order approximation to the molecular description, should be followed by an accurate site-site MCT approach [32] or by a full molecular MCT approach [34]. Theoretical development along these two lines are taking place at a fast pace and in the near future accurate theoretical predictions should be available for the quantities studied in this article. For the present time, we can only state that the characteristic MCT scenario appears able

to describe the dynamics of this simple, yet complete, molecular model.

## VI. ACKNOWLEDGMENT

We acknowledge financial support from the INFN PAIS 98, PRA 99 and *Iniziativa Calcolo Parallelo* and from MURST PRIN 98.

- 
- [1] W. Kob and H. C. Andersen, Phys. Rev. E **51**, 4626 (1995); *ibid.* Phys. Rev. E **52**, 4134 (1995).
- [2] M. Nauroth and W. Kob, Phys. Rev. E **55**, 675 (1997).
- [3] F. Sciortino, P. Gallo, P. Tartaglia, S.-H. Chen, Phys. Rev. E **54**, 6331 (1996); P. Gallo, F. Sciortino, P. Tartaglia, and S.-H. Chen, Phys. Rev. Lett. **76**, 2730 (1996).
- [4] F. Sciortino, L. Fabbian, S.-H. Chen, and P. Tartaglia, Phys. Rev. E **56**, 5397 (1997).
- [5] M. C. Ribeiro and P. A. Madden, J. Chem. Phys. **108**, 3256 (1998) and references therein.
- [6] B. Doliwa and A. Heuer, Phys. Rev. E **61**, 6898 (2000).
- [7] Lai S. K. Lai and G. F. Wang Phys. Rev. E **58**, 3072 (1998).
- [8] S. Kämmerer, W. Kob and R. Schilling, Phys. Rev. E **56**, 5397 (1997).
- [9] A. Heuer, Phys. Rev. Lett. **78**, 4051 (1997) ; S. Buechner and A. Heuer, Phys. Rev. E. **60**, 6507 (1999).
- [10] S. Sastri, P. Debenedetti and F. Stillinger, Nature, **393**, 554 (1998).
- [11] F. Sciortino, W. Kob and P. Tartaglia, Phys. Rev. Lett. **83**, 3214 (1999).
- [12] C. Donati, F. Sciortino, and P. Tartaglia, Phys. Rev. Lett. **85**, 1464 (2000).
- [13] E. La Nave, A. Scala, F.W. Starr, F. Sciortino and H.E. Stanley, Phys. Rev. Lett. **84**, 4605 (2000).
- [14] L. Angelani, R. Di Leonardo, G. Ruocco, A. Scala, F. Sciortino, cond-mat/0007241; *ibid.* Phys. Rev. Lett. **85**, 5356 (2000).
- [15] W. Götze, in *Liquids, Freezing and Glass Transition*, ed. J.P. Hansen, D. Levesque and J. Zinn-Justin, Les Houches Session LI, 1989 (North-Holland, Amsterdam, 1991).
- [16] W.Götze, J. Phys. Condens. Matter **11**, A1 (1999).
- [17] F. Sciortino and W. Kob, cond-mat/0008024; *ibid.* Phys. Rev. Lett. in press (2001).
- [18] L. Fabbian, F. Sciortino, F. Thiery and P. Tartaglia, Phys. Rev. E **57**, 1485 (1998).
- [19] L. Fabbian, A. Latz, R. Schilling, F. Sciortino, P. Tartaglia, and C. Theis, Phys. Rev. E **60**, 5768 (1999).
- [20] C. Theis, F. Sciortino, A. Latz, R. Schilling, P. Tartaglia, cond-mat/0003508; *ibid.* Phys. Rev. E **62**, 1856 (2000)
- [21] A. Winkler, A. Latz, R. Schilling, C. Theis, cond-mat/0007276.
- [22] B. J. Alder and T. E. Wainwright, J. Chem. Phys. **27**, 1208 (1957).
- [23] L.J. Lewis and G. Wahnström, Phys. Rev. E **50**, 3865 (1994).
- [24] D. J. Plazek, C. A. Bero, I. C. Chay, J. Non-Cryst. Solids **172-174**, 181-190 (1994).
- [25] W. Petry, E. Bartsch, F. Fujara, M. Kiebel, H. Sillescu, and B. Farago, Z. Phys. B **83**, 175-184 (1991).
- [26] J. Wuttke, M. Kiebel, E. Bartsch, F. Fujara, W. Petry, H. Sillescu, Z. Phys. B **91**, 357-365 (1993).
- [27] E. Bartsch, F. Fujara, J. F. Legrand, W. Petry, H. Sillescu and J. Wuttke, Phys. Rev. E **52**, 738 (1995).
- [28] A. Tölle, J. Wuttke, F. Fujara, and H. Schober, Phys. Rev. E **56**, 809 (1997).
- [29] C. Masciovecchio, G. Monaco, G. Ruocco, F. Sette, A. Cunsolo, M. Krisch, A. Mermet, M. Soltwisch, and R. Verbeni, Phys. Rev. Lett. **80**, 544 (1998).
- [30] G. Monaco, C. Masciovecchio, G. Ruocco, and F. Sette, Phys. Rev. Lett. **80**, 2161 (1998).
- [31] G. Monaco, D. Fioretto, C. Masciovecchio, G. Ruocco, and F. Sette, Phys. Rev. Lett. **82**, 1776 (1999).
- [32] S.-H. Chong and F.Hirata, Phys. Rev. E **58**, 6188 (1998); Phys. Rev. E **58**, 7296 (1998); Phys. Rev. E **57**, 1691 (1998).
- [33] T. Franosch, M. Fuchs, W. Götze, M.R. Mayr and A.P. Singh, Phys. Rev. E **56**, 5659 (1997).
- [34] R. Schilling and T. Scheidsteger, Phys. Rev. E **56**, 2932 (1997); T. Scheidsteger and R. Schilling, Phil. Mag. B **77**, 305 (1998); C. Theis, Diploma Thesis, Johannes Gutenberg Universität Mainz (1997).
- [35] G. Wahnström and L. J. Lewis, Prog. Theor. Phys. Suppl. **126**, 261 (1997).
- [36] J.-L. Barrat, W. Götze, and A. Latz, J. Phys.: Condens. Matter **1**, 7163 (1989).
- [37] J.P. Hansen and I.R. McDonald, *Theory of Simple Liquids* (Academic Press, London, 1986), 2nd Edition.
- [38] A. P. Singh, *Die Störung der  $\beta$ -Dynamik durch oszillierende Moden*, Diploma thesis, TU München, 1995.
- [39] S. Mossa, R. Di Leonardo, G. Ruocco, M. Sampoli, Phys. Rev. E **62**, 612 (2000). S. Mossa et al (preprint).
- [40] F. Sciortino and P. Tartaglia, J. Phys.: Condens. Matter **11**, A261 (1999).
- [41] J. Horbach and W. Kob, Phys. Rev. B **60**, 3169 (1999).
- [42] F. W. Starr, S. Harrington, F. Sciortino, and H. E. Stanley, Phys. Rev. Lett. **82**, 3629 (1999).
- [43] M. Fuchs, I. Hofacker and A. Latz, Phys. Rev. A **45**, 898 (1992).
- [44] W. Gotze, A. P. Singh, Th. Voigtmann Phys. Rev. E **61**, 6934 (2000).
- [45] L. Fabbian, F. Sciortino and P. Tartaglia, J. Non-Cryst. Solids **235-237**, 350 (1998).
- [46] F. Sciortino, Chem. Phys. **258**, 295-302 (2000).
- [47] C. Theis and R. Schilling, J. Non-Cryst. Solids **235-237**, 106 (1998).
- [48] D. Morineau, C. Alba-Simionesco, J. Chem. Phys. **109**, 8494 (1998); D. Morineau, C. Alba-Simionesco, M.C. Bellissent-Funel and M.F. Lautie, Europhys. Lett. **43**, 195 (1998).
- [49] L. Fabbian, A. Latz, R. Schilling, F. Sciortino, P. Tartaglia, and C. Theis, Phys. Rev. E **62**, 2388 (2000).
- [50] C. Alba-Simionesco, A. Tölle, D. Morineau, B. Farago

and G. Coddens, “*de Gennes*” narrowing in supercooled molecular liquids: Evidence for center-of-mass dominated slow dynamics preprint (2000).

- [51] The wavevector dependence of the triplet density fluctuations  $\langle \rho_s(\mathbf{k})\rho_s(\mathbf{p})\rho_s(\mathbf{q}) \rangle$  fully determines the wavevector dependence of the static structure factor (i.e. the pair density fluctuations) via the Born-Green-Yvon (BGY) equation [52]. It is easy to show that the approximation  $c_3 = 0$ , when used in conjunction with the BGY equation, produces an implicit equation for the static structure factor which does not depend on density. The approximation  $c_3 = 0$  should not be used in the hydrodynamic limit.
- [52] A. N.H.March and M.P.Tosi, Atomic dynamics in liquids, p.23 Dover (NY) 1991.

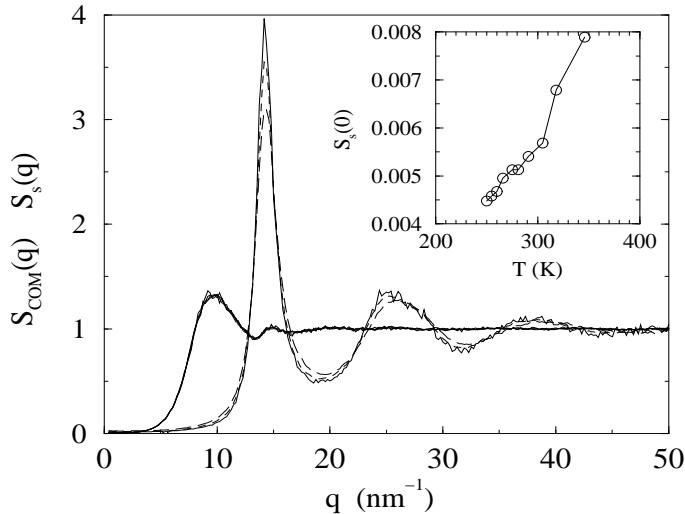


FIG. 1.  $S_s(q)$  and  $S_{COM}(q)$ . For clarity reasons, only data for  $T = 255K$ ,  $T = 281K$  and  $T = 346K$  are shown. Note that  $S_{COM}(q)$  is temperature independent, while for the  $S_s(q)$ , the height of the first peak increases on cooling. The inset shows the  $T$ -dependence of the structure factor at  $q = 0$ .

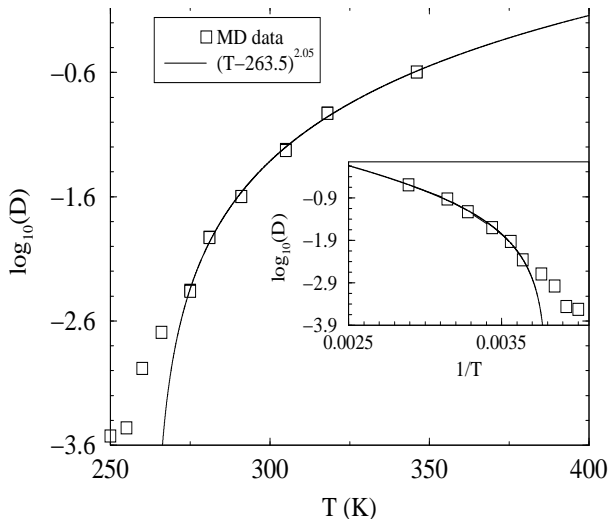


FIG. 2. Temperature dependence of the diffusion coefficient, evaluated from the long time limit of the mean square displacement. The inset show the same data as a function of  $1/T$ .

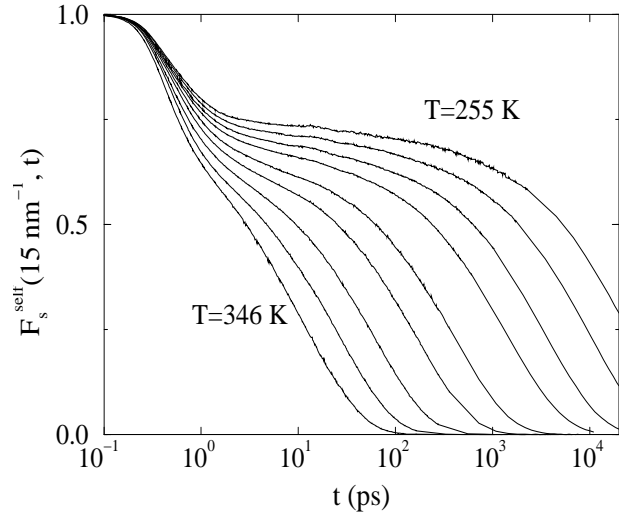


FIG. 3. Site self-correlation function for all studied temperatures at  $q = 15 \text{ nm}^{-1}$  (the location of the first maximum of the site structure factor).

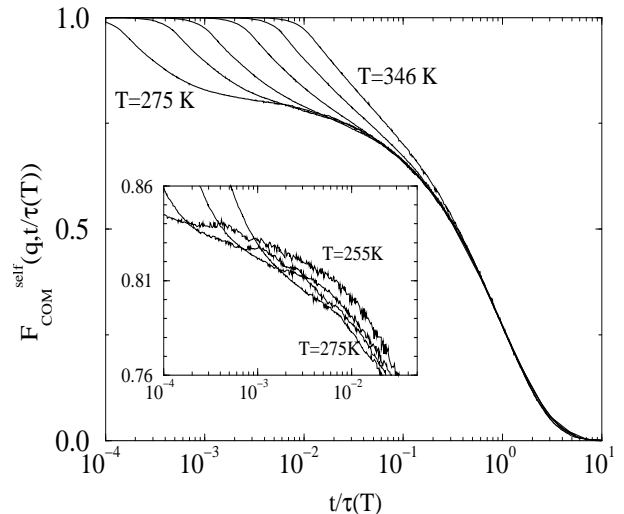


FIG. 4.  $\alpha$ -scaling for the COM self-correlation function for different  $T$  at  $q = 13 \text{ nm}^{-1}$  — the position of the first minimum in  $S_{COM}(q)$ . The main plot shows, from right to left  $T = 346, 318, 305, 291, 281, 275K$ . The inset shows the region around the plateau for  $T = 275, 266, 260, 255K$ .

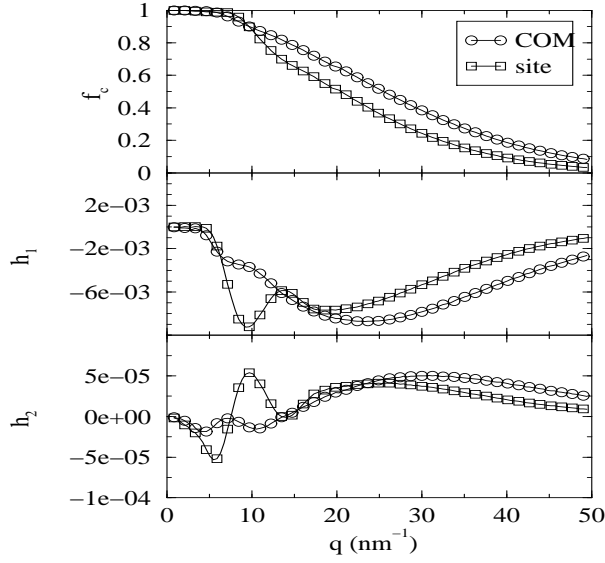


FIG. 5. Wavevector dependence of the fitting parameters according to the Von Schweidler law (Eq. 14) for the self correlation functions  $F_s^{self}(q, t)$  and  $F_{COM}^{self}(q, t)$ .  $T = 275K$ .

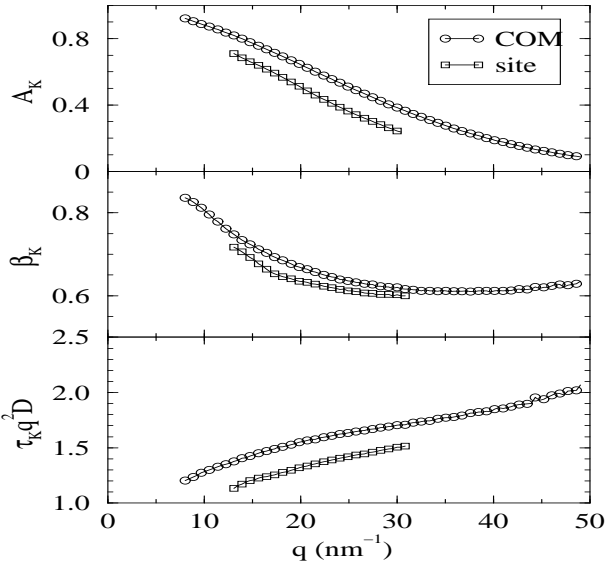


FIG. 6. Wavevector dependence of the fitting parameters according to the stretched exponential form (Eq. 16) for  $F_s^{self}(q, t)$  and  $F_{COM}^{self}(q, t)$ .  $T = 275K$ .

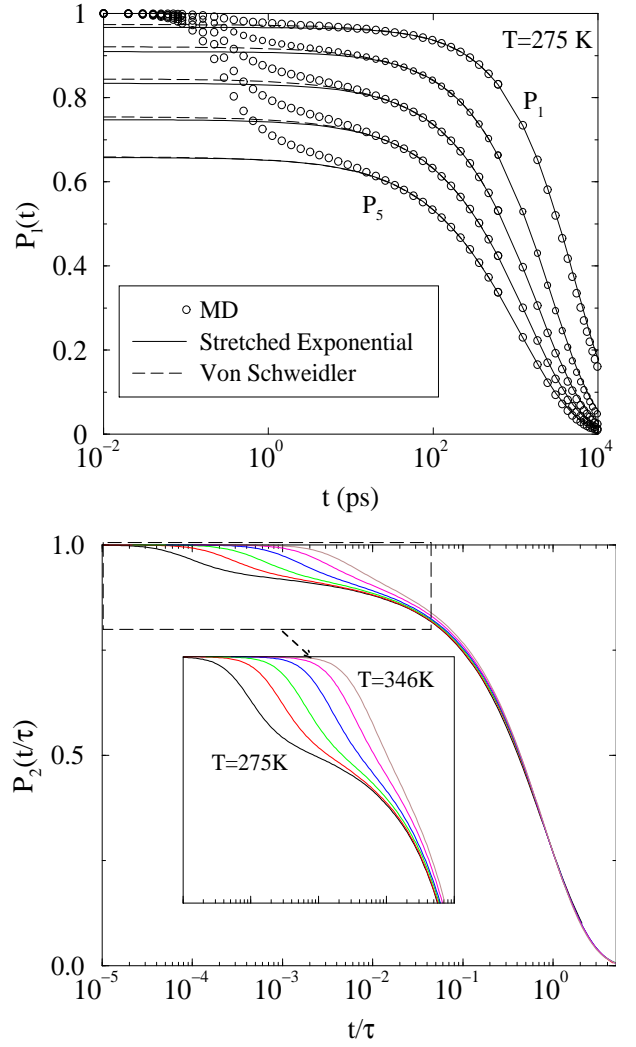


FIG. 7. (top) Time dependence of the first five Legendre polynomials at  $T = 275K$ . (bottom) Time-Temperature superposition for the second-order Legendre polynomial.



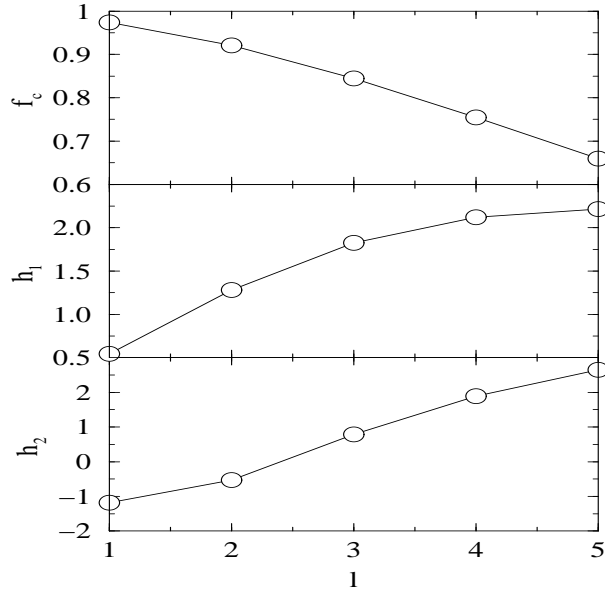


FIG. 8. Fitting parameters according to the Von Schweidler law of the first five Legendre polynomials

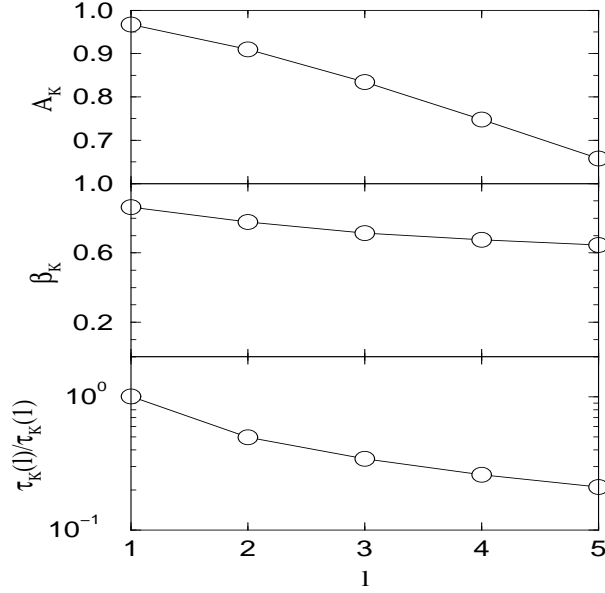


FIG. 9. Legendre's order dependence of the fitting parameters according to the stretches exponential form (Eq. 16)

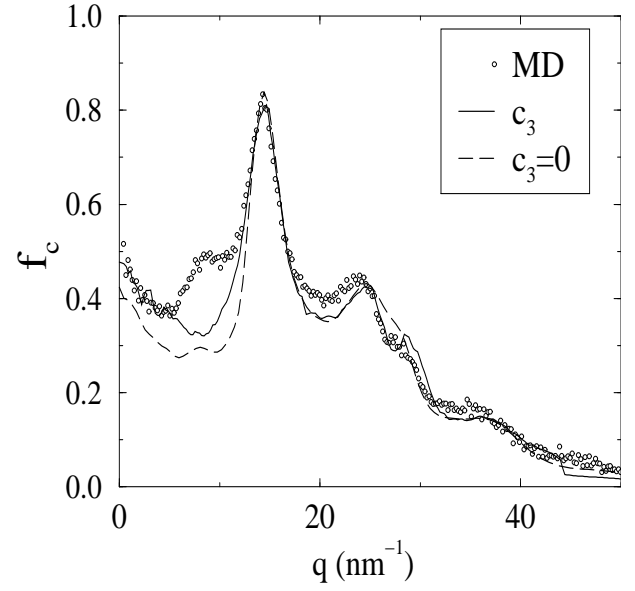


FIG. 10. Wavevector dependence of the non-ergodicity factor. The MD data has been calculated as fitting parameters according to the Von Schweidler law (14) The full and dashed lines are the prediction of the MCT using the site structure factor as input and including or excluding the  $c_3$  contribution.

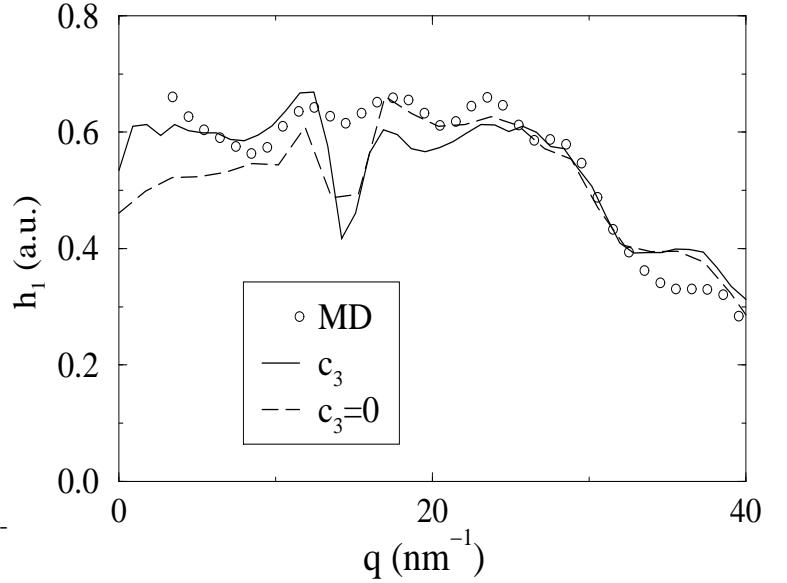


FIG. 11. Wavevector dependence of the amplitude  $h_1$ . The MD data (symbols) are the result of the fit according to the Von Schweidler law (Eq. 14). Lines are MCT predictions.

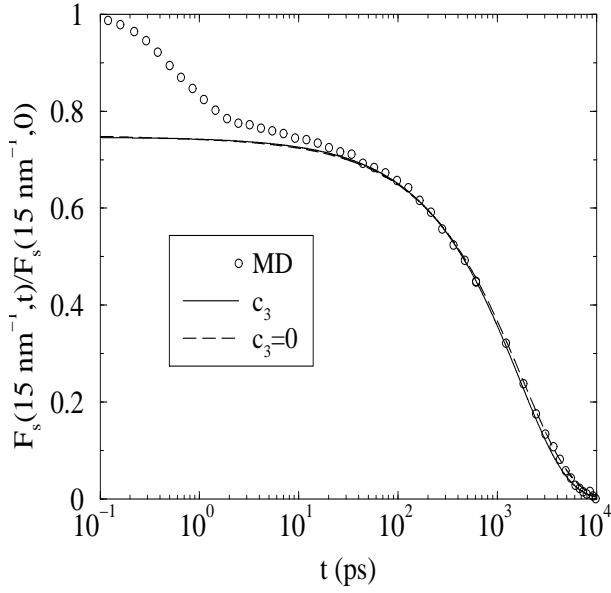


FIG. 12. Site-site  $\alpha$ -relaxation dynamics at the peak of the structure factor at  $T = 275K$ . Symbols are MD results, lines are MCT predictions.

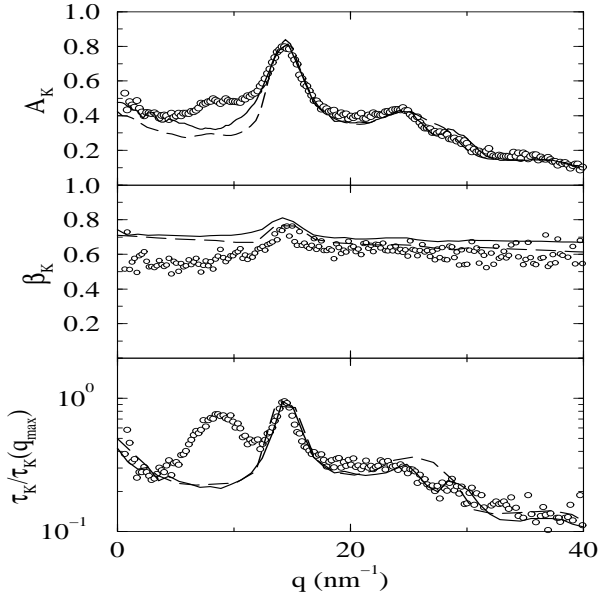


FIG. 13. Wavevector dependence of the fitting parameters according to the stretched exponential form (Eq. 16) for the normalized  $F_s(q, t)$ . Symbols are MD results. The full and dashed lines are the prediction of the MCT using the site structure factor as input and including or excluding the  $c_3$  contribution.

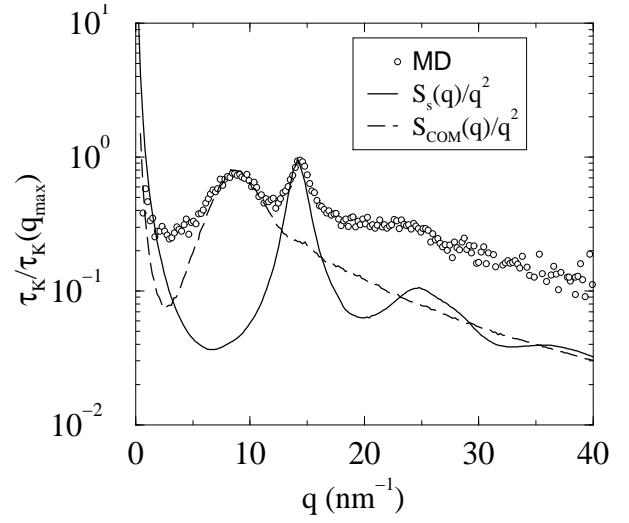


FIG. 14. Comparison of the wavevector dependence of the  $\alpha$ -relaxation time with the de Gennes approximation for both site and COM.

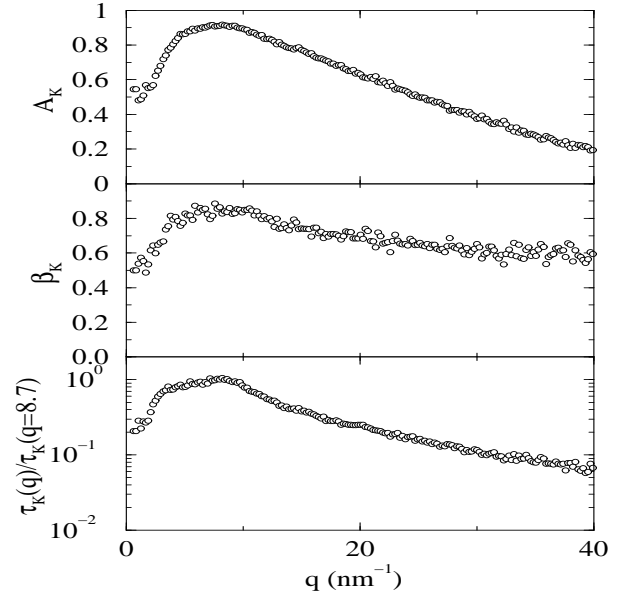


FIG. 15. Wavevector dependence of the fitting parameters according to the stretched exponential form (Eq. 16) for the normalized  $F_{COM}(q, t)$ .

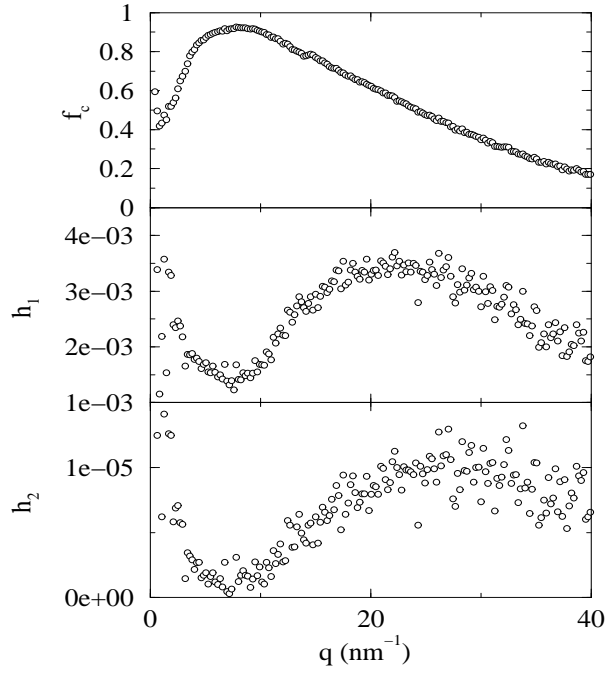


FIG. 16. Wavevector dependence of the fitting parameters according to Eq. 14 for the normalized  $F_{COM}(q, t)$ .

TABLE I. For each temperature we list the diffusion coefficient, the density, the averages of the internal energy and of the external pressure and the length of the simulation time after the equilibration.

$T$ (K)	$D$ ( $10^{-5} \text{cm}^2/\text{s}$ )	$\rho$ ( $\text{g}/\text{cm}^3$ )	U ( $\text{kJ}/\text{mol}$ )	P (MPa)	$t_{sim}$ (ns)
255	0.00035	1.0851	-77.6	0.02	41
260	0.0010	1.0822	-77.3	-1.2	52
266	0.0020	1.0790	-77.0	-1.0	37
275	0.0043	1.0763	-76.5	5.4	37
281	0.012	1.0703	-75.8	0.7	14
291	0.025	1.0650	-75.2	2.0	16
305	0.059	1.0554	-74.1	1.0	5
318	0.12	1.0439	-72.9	-2.3	7
346	0.25	1.0269	-71.0	-13.0	6